BY-NC

Marek Stanisław Węglowski, Yu Ming Zhang

Usability of welding arc electromagnetic radiation in diagnosing a MAG welding process

Abstract: The study presents ideas and test results related to an unconventional method of MAG welding process monitoring making use of welding arc radiation in the visible range. The experiments conducted indicate the direction of further research on the phenomenon of welding arc radiation and the possibilities of using it for on-line monitoring of other welding processes. The recording of spectral distribution was made using a spectrophotometric card. The stability of a welding process was assessed using the least squares sum remainder method. Recorded signals were modelled using polynomials and the optimum polynomial order was selected using the F-test method. The study presents the impact of welding current intensity and of a filler metal type on the distribution of welding arc visible radiation spectrum.

Keywords: MAG welding, welding arc radiation, monitoring;

Introduction

Typical welding processes such as arc welding, laser beam welding or electron beam welding can be perceived as a system having inputs and outputs. Theoretically, all the properties of a weld, and those of HAZ, are treated as outputs and must meet strictly specified requirements, e.g. those related to mechanical properties or microstructure. In turn, adjustable welding process parameters, e.g. welding current, arc voltage, filler metal feeding rate and welding rate can be treated as inputs and should be appropriately selected in order to ensure required joint properties. Therefore, the main task of welding personnel (engineers) is to select a proper welding process and adjust welding parameters, i.e. input data to a system, in order to obtain a required welding joint quality, i.e. required values at the output of a system. To this end it is necessary to carry out experimental tests such as making test joints, conducting required NDT and destructive testing as well as specifying the range of values at the output of a system, i.e. joint properties. In many applications the adjustment of proper parameters (input data) ensures obtaining a joint quality level (output data) as required by related regulations and standards. However, it should be noted that welding conditions such as the geometry of a joint and the chemical composition of a base metal should be contained within a range, for which experimental tests have been carried out and for which welding parameters have been adjusted. If welding conditions change and no longer correspond to a range taken into consideration, joint properties may also diverge from

dr inż. Marek St. Węglowski (PhD Eng.) - Instytut Spawalnictwa, Testing of Materials Weldability and Welded Constructions Department; Prof. Yu Ming Zhang - Centre for Manufacturing, University of Kentucky, Lexington, USA

BY-NC

adopted assumptions – output data will be outside the range. A welding process treated as a system (Fig .1) has inputs depending on welding conditions (welding parameters adjusted with a device) which can be changed and controlled as well as disturbances - uncontrolled changes of welding parameter values or welding process disturbances caused by e.g. impurities on the surfaces of elements being welded [1].

One of the methods informing about the proper operation of a system is welding pro-

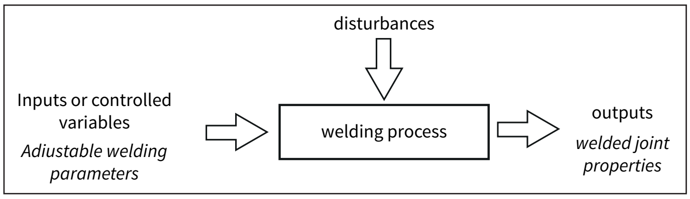

Fig. 1. Welding process as a system [1]

cess monitoring which might help limit the use of NDT, and thus significantly reduce production costs. On-line welding process monitoring methods should become part of the whole production system. Depending on the place at which a monitoring process is carried out, there can be three groups of systems which control [2]:

– preparation of a joint before welding, e.g. weld groove geometry inspection,
– welding process during making a joint,
– finished joint prior to NDT.

Monitoring welding processes (during making a joint) can be carried out using conventional and unconventional methods. The first group includes the measurements and recordings of signals coming from a welding circuit, usually welding current and welding arc voltage [3]. Less popular are the measurements of welding rate, shielding gas flow intensity and those of filler metal feeding rate [1]. These methods are cheap and usually do not require the use of complicated measuring systems. However, it should be noted that in the case of recording and archiving many data collected from various test rigs, requirements related to the system increase both as to its efficiency and data transfer methods. Presently developed and implemented are multi-rig systems [4]. In many cases, conventional methods must be supported or even replaced with unconventional ones, which are based mainly on the measurements of signals emitted from a welding area. An arc welding process can be diagnosed with unconventional methods, for instance, involving systems based on measurements of sounds [3, 5] or arc electromagnetic radiation intensity [6, 7, 8]. Quick filming methods are also a very useful technique [1, 9], particularly if supported by advanced image analysis methods [10]. Welding process stability assessments can be conducted with numerous methods. The most popular of them include the time and frequency analysis of recorded signals [4, 11]. Often used are also artificial neural networks [3, 12], fuzzy set methods [13] and genetic algorithms [14].

This study explores arc electromagnetic radiation intensity used for controlling a MAG welding process. Radiation spectrum distribution was recorded using a spectrophotometric card. The stability of a process was determined using the least squares method. The objective of the study was to determine the usability of welding arc electromagnetic radiation in diagnosing a MAG welding process. Elements taken into consideration were the changes of technological parameters and the impact of welding process disturbances.

Testing methodology

Tests were carried out on an automatic MIG/MAG welding station. The scheme of the station along with information flow directions is presented in Figure 2. The distribution of a welding arc radiation spectrum was recorded with a PCI 2000 ISA-A spectrophotometric card, based on a CCD Sony model ILX511 converter. The card operated in a range from 340 to 860 nm and was PC-controlled.

The sampling frequency of the spectrophotometric card was 3 kHz. A welding arc was treated as a spot light source. The tests involved the measurements of welding current, welding

BY-NC

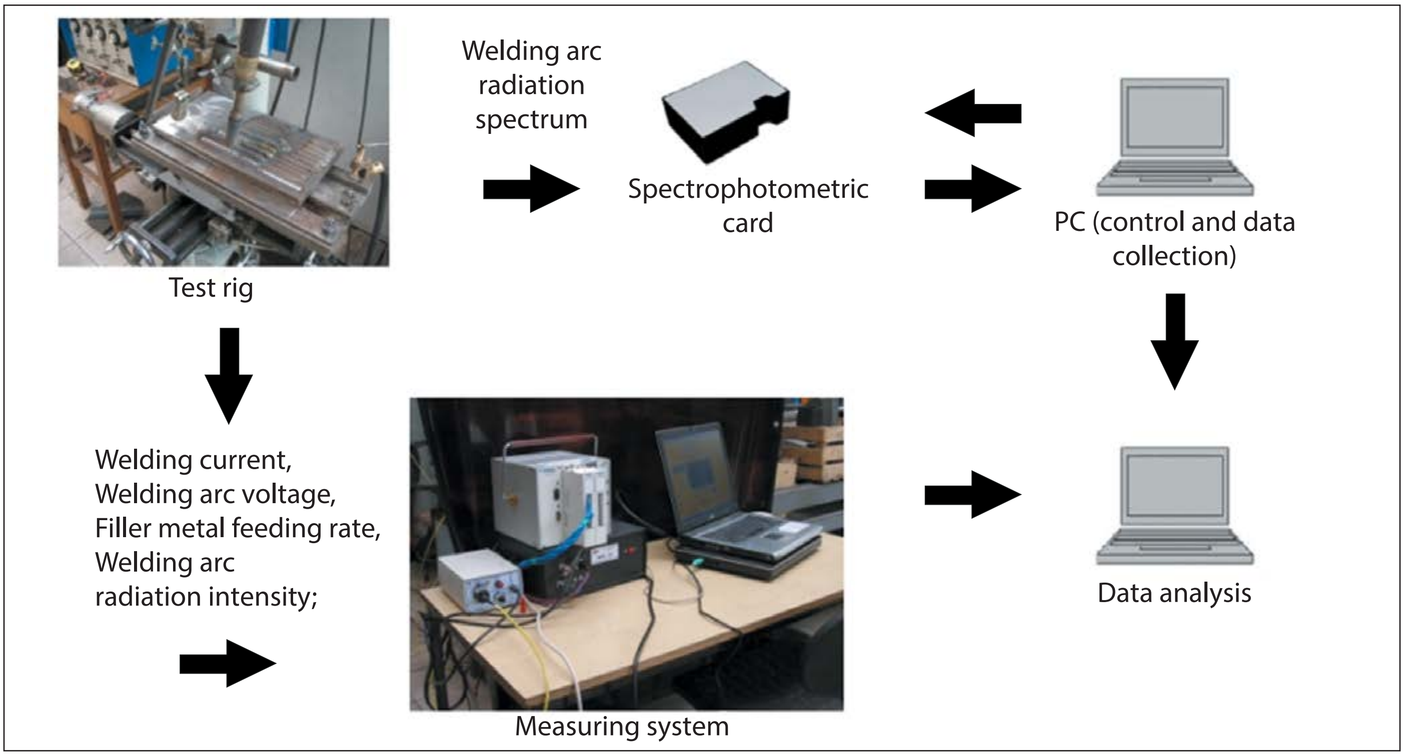

Fig. 2. Scheme of test rig with information flow directions

arc voltage, filler metal feeding rate and arc radiation intensity with a frequency of 20 kHz. Current intensity was measured with a PR 1001 clamp meter, arc voltage was measured with an LV 25P converter, and a filler metal feeding rate was measured using an E21 MPL10 converter. A PIN BPW34 photodiode was used for radiation intensity measurements. Signals from a welding circuit were recorded with a IPP-2 monitoring device, designed at Instytut Spawalnictwa [15]. The device is based on a National Instruments SCXI measurement system consisting of a module composed of SCXI-1125 input signal cards and an NI DAQ 6036 E measuring card.

During testing the impact of welding current intensity on the distribution of an arc radiation spectrum, the welding torch remained unmoved and the test plate was shifted. During testing the impact of disturbances on electromagnetic radiation the plate remained unmoved and the welding torch was shifted. In both cases the optical system remained unmoved in relation to the welding torch. The distribution of a spectrum was recorded while making overlay welds on a 20 mm thick S235JR grade steel plate. The tests also involved the use of an OK Autrod 12.64 (PN-EN ISO 14341 G4SI1) filler metal wire by ESAB (dia. 1.2 mm). A shielding gas used in the tests was Ferromix C18 (PN-EN ISO 14175 - M21) by Messer. The tests were carried out with welding parameters presented in Table 1. The

Table 1. MAG method welding parameters

No.	Welding current [A]	Arc voltage [V]	Overlay welding rate [cm/min]	Overlay welding linear energy [kJ/cm]
I	104	16.5	27	4.8
II	130	18.0	30	6.5
III	235	25.5	40	16.7

Remarks: Shielding gas flow rate 14 l /min. Parameters were adjusted experimentally for ensuring proper overlay weld shape

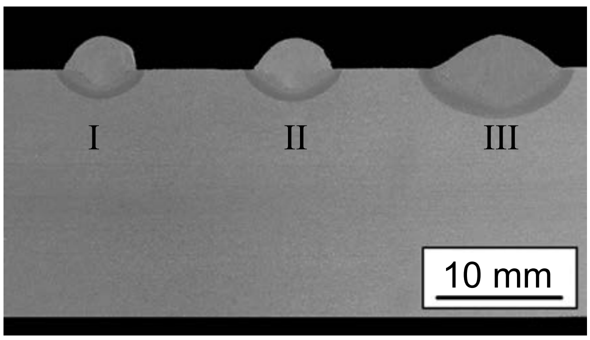

Fig. 3. Macrostructure of overlay welds made with parameters presented in Table 1

BY-NC

Table 2. Characteristics of filler metal wires

No.	Trade name/ manufacturer	Designation according to standard	Chemical composition [%]	Intended use
I	OK Autrod 12.64, ESAB	PN-EN ISO 14341 - A-G4Si1	C – 0.10; Mn – 1.7; Si – 1.0	Copperised solid electrode wire with manganese and silicon additions, intended for MIG/MAG (GMAW) welding of unalloyed steels, with a minimum yield point below 460 MPa.
II	A 101, Interweld	PN-EN 13347-CF309G PN-EN ISO 24373 Cu6100	Al – 8.0; Mn – 0.3; Cu – remainder	Wire for welding and overlay welding of aluminium bronzes, for joining aluminium bronzes with steels, for joining steels with copper and its alloys.
III	Robodur K 450, Welding Alloys	PN-EN 14700 - T Fe2	C – 0.40; Mn – 1.5; Si – 0.70 Cr – 2.50; Mo – 0.50	Wire for rebuilding (regeneration overlay welding) for rolled and forged elements
IV	A 7 Buehler	PN EN ISO 14343 – G 18 8 Mn	C-0.08, Si-0.9; Mn-7.0; Cr-19.2; Ni-9.0	Alloy wire for welding and overlay welding, for making dissimilar joints and buffer layers.

welding power source was an OZAS MAGOMIG550 device with an OZAS ZP-15 filler metal wire feeder. Figure 3 presents the macrostructures of overlay welds obtained.

This study also involved the determination of the impact of a filler metal on a welding arc radiation spectrum. Four filler metal wires differing in their chemical composition were selected for the tests (Table 2). The tests were carried out on a 20 mm thick S235JR grade steel sheet.

Prior to overlay welding the surface of the plate was cleaned mechanically. The tests were carried out with the following technological conditions:

– welding current 160 A,
– welding arc voltage 21.2 V,
– shielding gas flow rate 12 l/min,
– overlay welding rate 18 cm/min,
– filler metal wire diameter 1.2 mm.

The results of macroscopic tests of overlay welds obtained are presented in Figure 4. Following grinding, the samples were etched with the Adler's reagent.

The second stage of the tests involved the determination of the impact of welding process disturbances on the radiation of a welding arc in the MAG method. The disturbance to a welding process consisted in placing a filler metal (a filler metal wire section with a diameter of 2.4 mm) in a weld groove. The purpose of placing the filler metal was to trigger welding imperfections. Figure 5 presents the view of a joint made after causing the disturbance. The areas in which the filler metal was placed are marked. A welded joint was made with the following welding parameters:

– welding current 160 A,
– welding arc voltage 21.2 V,
– welding rate 18 cm/min,
– joint thickness 4 mm, V-bevelled.

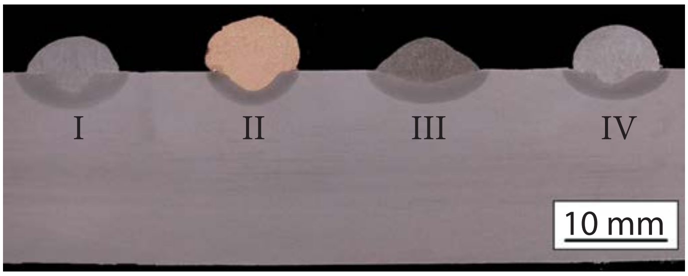

Fig. 4. Macrostructure of overlay welds made with welding current of 160 A using filler metals wires presented in Table 2

BY-NC

Fig. 5. View of welded joint made after introducing disturbance in the form of filler metal placed in weld groove

Test results and analysis

The first stage of the tests aimed to determine the impact of welding current intensity and that of a filler metal type on the distribution of welding arc electromagnetic radiation spectrum in the range 340 – 860 nm. The distribution of MAG welding arc radiation spectrum in the wavelength range 360-500 nm is presented in Figure 6, in the range 480-700 nm in Figure 7, and in the range 680-800 nm in Figure 8. Diagrams are presented in a semi-logarithmic scale.

As presented in Figures 6, 7 and 8, an increase in welding current intensity (linear energy) causes an increase in welding arc radiation intensity in the whole range measured. In order to calculate the characteristic quantities of a spectral line (intensity, central line and half-value width FWHM - Full Width at Half Maximum) each single spectral line was modelled with three functions, i.e. Lorentz, Gauss and Voigt functions (Fig. 9). Modelling was carried out for single spectral lines as well as for many lines simultaneously. Matching the spectral lines with proper elements was based on the atlases of spectral lines. The tests results revealed that metal vapours are the main source of welding arc radiation in the MAG. Among the spectral lines the lines corresponding to iron and manganese were selected. No spectral lines connected with the shielding gas were detected. A detailed spectrum distribution

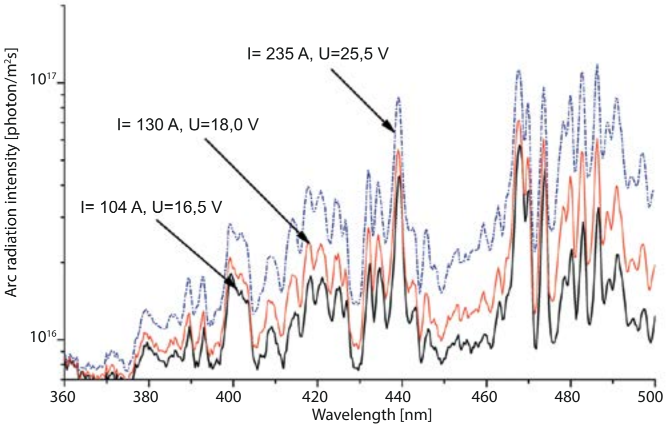

Fig. 6. Impact of welding current intensity on distribution of welding arc radiation spectrum in wavelength range 360-500 nm. Semi-logarithmic scale

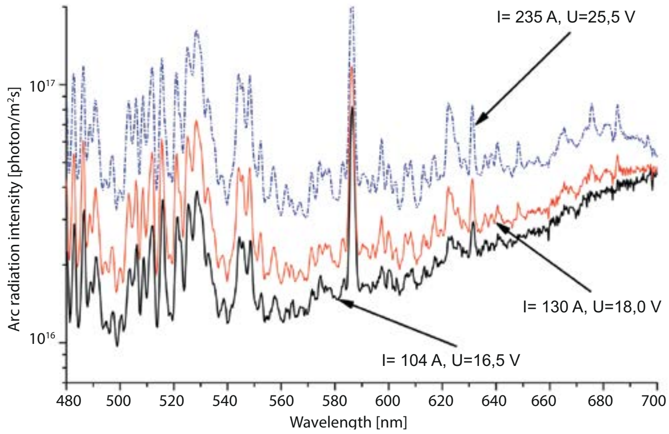

Fig. 7. Impact of welding current intensity on the distribution of welding arc radiation spectrum in wavelength range 480-700 nm. Semi-logarithmic scale

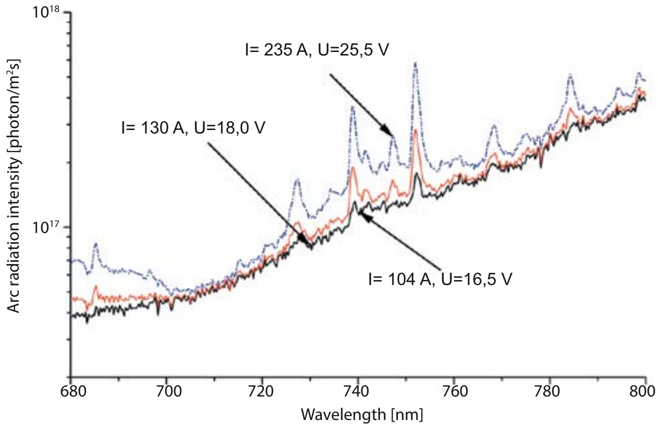

Fig. 8. Impact of welding current intensity on the distribution of welding arc radiation spectrum in wavelength range 680-800 nm. Semi-logarithmic scale

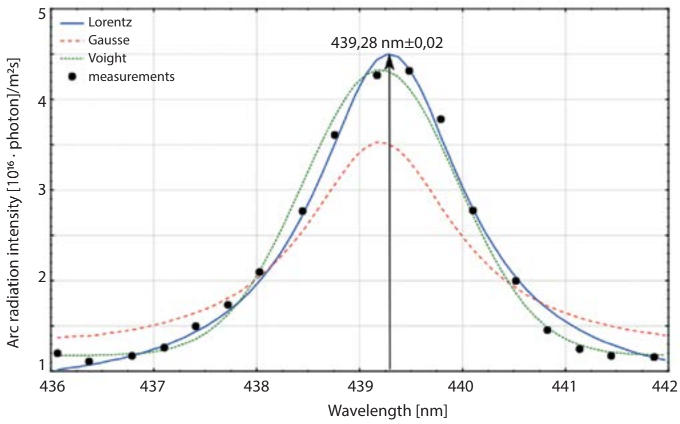

Fig. 9. Exemplary peak matched with Gauss, Lorentz and Voigt functions, I=130 A, U=18,0 V

BY-NC

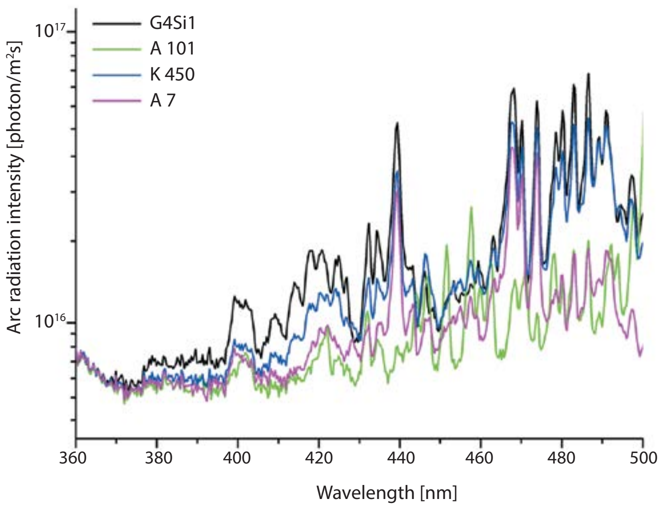

Fig. 10. Distribution of welding arc radiation spectrum in MAG method depending on filler metal wire in a wavelength range from 360 to 500 nm. Semi-logarithmic scale

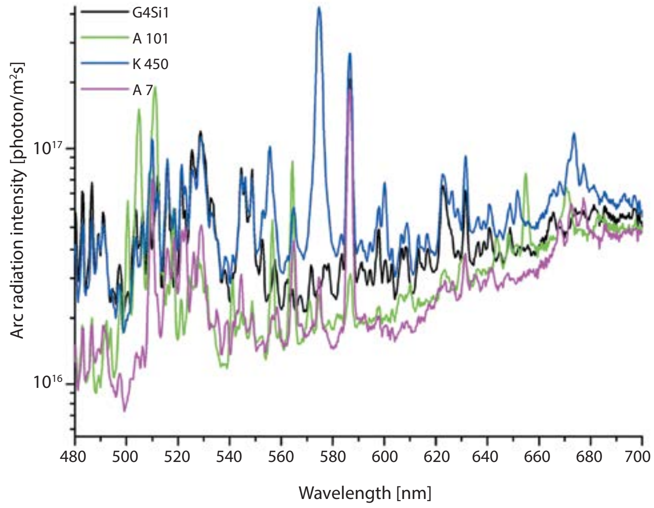

Fig. 11. Distribution of welding arc radiation spectrum in MAG method depending on filler metal wire in a wavelength range from 480 to 700 nm. Semi-logarithmic scale

analysis was presented in the publication [7]. The results of the measurements of welding arc spectrum distribution depending on the type of a filler metal wire are presented in Figures 10-12.

As can be seen in Figures 10-12, the type of a filler metal significantly affects the radiation of a welding arc which results from the fact that in welding with a filler metal some liquid metal coming from the tip of a filler metal wire is supplied to the area of an arc. The emission of the ions of chemical elements composing a given filler metal wire contributes to the overall emission of welding arc radiation.

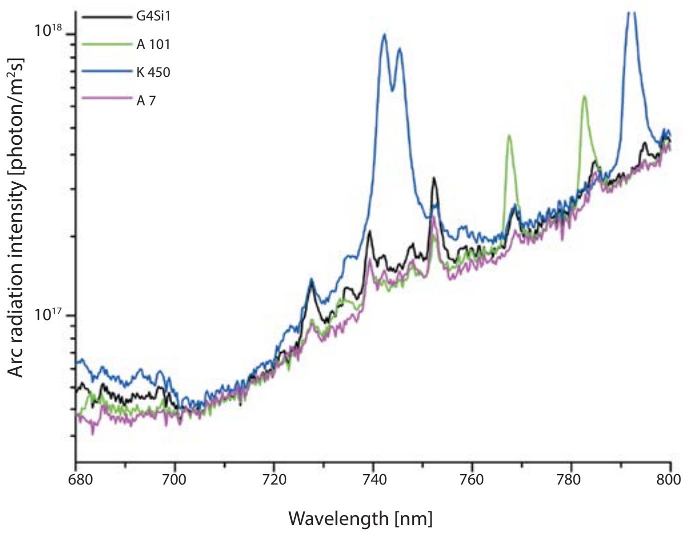

Fig. 12. Distribution of welding arc radiation spectrum in MAG method depending on filler metal wire in a wavelength range from 680 to 800 nm. Semi-logarithmic scale

The second stage of the tests aimed at the determination of welding process disturbances on arc radiation intensity. Figure 5 presents the view of a test plate.

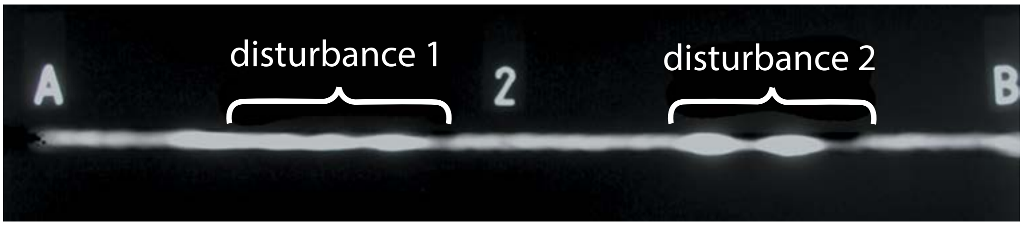

Fig. 13. Radiogram of MAG welded joint after introducing disturbance in the form of filler metal

In the area of disturbance 1, it was possible during metallographic tests to observe excessive root penetration as well as no penetration. In turn, the area of disturbance 2 revealed the incomplete filling of a weld groove. The results of radiographic tests in the form of a welded joint radiogram

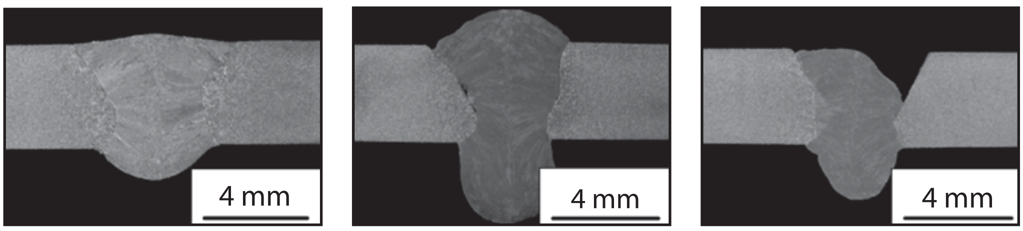

Fig. 14. Macrostructure of welded joint with characteristic areas. Etchant- Adler

BY-NC

are presented in Figure 13. They revealed that the joint was free from other welding imperfections. Figure 14 presents the results of macroscopic metallographic tests of the characteristic areas of a joint. Figure 15 presents the waveform of welding arc radiation intensity with marked areas of disturbances.

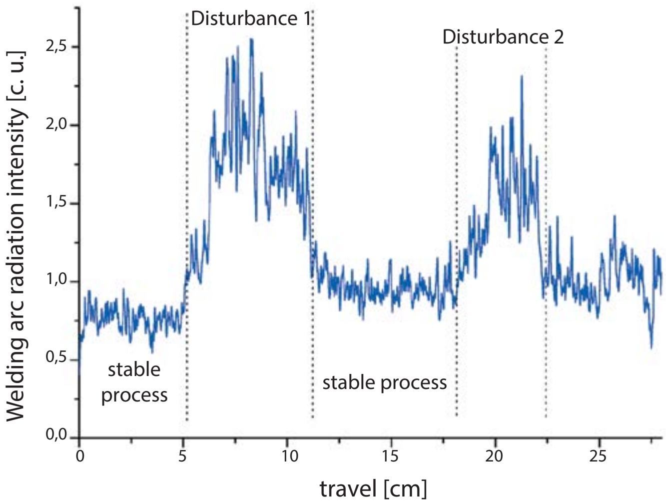

Fig. 15. Recorded waveform of welding arc radiation intensity during making a joint – unstable process, disturbance in the form of filler metal in weld groove, c.u. – conventional units

The assessment of the stability of a welding process based on the measurement of welding arc radiation intensity involved the least squares method [16,17]. A signal was modelled using a third-order polynomial:

$$y=a_0 + a_1x + a_2x^2 + a_3x^3 + \varepsilon \quad (1)$$

where:
y – arc radiation intensity,
x – time,
a_i – constants,
ε – difference between a real value and a remainder.
In order to calculate the residual it is necessary to solve a matrix equation:

$$Y \approx X\beta \quad (2)$$

where:
Y– matrix of arc radiation intensity,
X – time matrix,
β – matrix of coefficients.

The residual is calculated using the following equation:

$$\varepsilon = \sqrt{\frac{(Y-\bar{Y})^T(Y-\bar{Y})}{2M+1}} \quad (3)$$

where:
2M+1 – number of samples used in the model.

During calculating equations (2) and (3) it was assumed that M=10, at a step of 100. The determination of places demonstrating the instability of a welding process was carried out by means of modelling with polynomials. The final stage of the modelling process was the selection of the optimum order of a polynomial. For this purpose the F-test method [18] was used. On the basis of previous assumptions concerning the least squares method, the residual εP determining the accuracy of modelling by means of polynomials:

$$\varepsilon_P = \sqrt{\frac{(\varepsilon-\bar{Y})^T(\varepsilon-\bar{Y})}{n}} \quad (4)$$

where
ε – remainder from equation 3,
Y – value of polynomial function,
n – number of data.

The matching of a function was carried out for 50 various polynomials. The residual εP was calculated in accordance with the equation (4). The impact of a polynomial order on the result of modelling (residual εP) is presented in Figure 16. The best results were obtained for the 28-order polynomial (Fig. 17). Figure 18 presents the result of modelling with the 28-order polynomial.

Summary

The study discusses the impact of MAG welding conditions on welding arc radiation. The tests conducted enable the formulation of the following conclusions:
- increase in linear energy causes an increase in welding arc radiation intensity,
- distribution of a welding arc radiation spectrum

BY-NC

in the MAG method depends on a the filler metal type,
- welding arc electromagnetic radiation is useful in diagnosing MAG welding processes,
- places demonstrating the instability of a welding process were detected using the least squares method; 28-order polynomial enabled the most accurate matching.

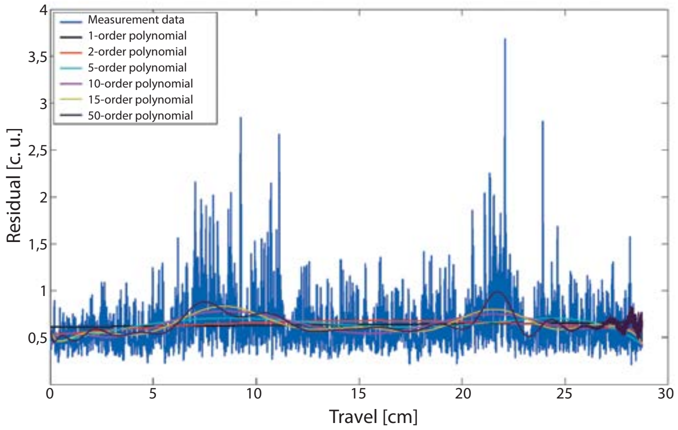

Fig. 16. Impact of polynomial order on matching with measurement data

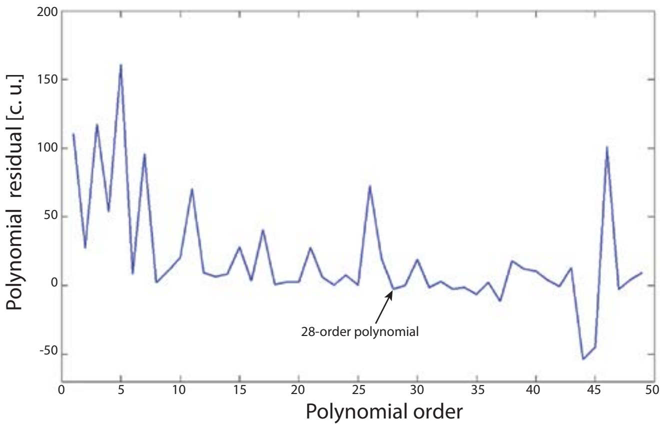

Fig. 17. Impact of polynomial order on remainder from matching

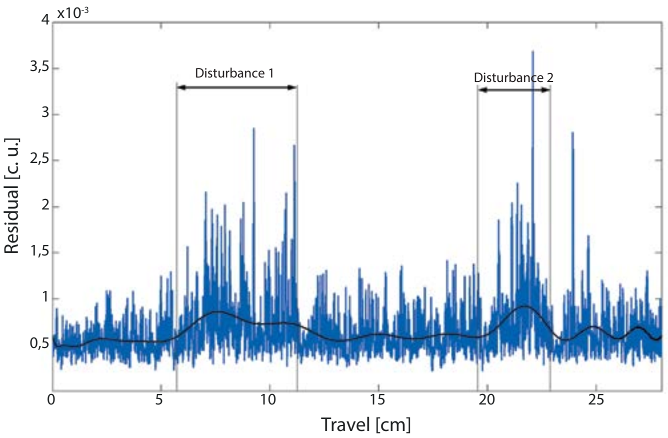

Fig. 18. Result of modelling using 28-order polynomial with marked areas of welding process instability

Acknowledgements

The research was partly funded by the Ministry of Science and Higher Education within research project no. 3 T10C 021 28 and the statutory activity of Instytut Spawalnictwa. Some research-related tests were carried out within the confines of Junior Fullbright Research Grant programme at University of Kentucky College of Engineering Center for Manufacturing Welding Research and Developed Laboratory.

References:

1. Zhang, Y. M. (2007). *Real time monitoring of welding processes.* Woodhead Publisher Limited.
2. Naidu, D.S., Ozcelnik, S. and Moore, K.L. (2003). *Modeling, sensing and control of Gas Metal Arc welding.* Elsevier, Amsterdam.
3. Luksa, K. (2012). *Przydatność sygnałów emitowanych przez elektryczny łuk spawalniczy do diagnozowania procesu spawania MAG. Monografia.* Wydawnictwo Politechniki Śląskiej, Gliwice.
4. Szubert, L., Skoczewski, P. and Welcel, M. (2010). *System rejestracji parametrów elektrycznych procesu spawania dla wielu stanowisk produkcyjnych.* Sprawozdanie z pracy statutowej ST-284/Fc-89, Instytut Spawalnictwa, Gliwice.
5. Saini, D. and Floyd S. (1998). An investigation of Gas Metal Arc welding sound signature for on-line quality control. *Welding Journal*, 77, (4), pp. 172-179.
6. Kovacevic, R., Węglowski, M.St. et al. (2012). *Welding process*. InTech, Rijeka.
7. Węglowski, M.St. (2008). Modelling and Analysis of Arc Light Spectrum in GMAW. *Welding Journal*, 87 (8), pp. 212-218.
8. Węglowski, M.S. (2009). Measurement of arc light spectrum in the MAG welding method. *Metrology and Measurement Systems*, 16 (1), pp. 143-159.
9. Węglowski, M.S., Yi, H. and Zhang Y.M. (2008). Relationship between wire feed speed and metal transfer in GMAW. *Journal*

BY-NC

of Achievements in Materials and Manufacturing Engineering, 29 (2), pp. 191-194.
10. Wang, Z.Z. and Zhang, Y.M. (2007). Image processing algorithm for automated monitoring of metal transfer in double-electrode GMAW. *Measurement Science and Technology*, 18, pp. 2048-2058.
11. Chu, Y.X., Hu, S.J., Hou, W.K., Wang, P.C. and Marin, S.P. (2004). Signature analysis for quality monitoring in short circuit GMAW. *Welding Journal,* 83 (12), pp. 336-343.
12. Smith, J. and Lucas, B. (1999). Putting intelligence into welding - rule based systems, fuzzy logic and neural networks. *Welding & Metal Fabrication,* 10, pp. 7-9.
13. Kim, Y. and Rhee, S. (2001). Development of an arc sensor model using a fuzzy controller in gas metal arc welding. *Measurement Science and Technology*, 12, pp. 534-541.
14. Köveš, A. and Golob, M. *A review of welding applications based on soft computing methods.* IIW Doc. No. XII-1806-04.
15. Węglowski, M.St., Mikno, Z., Welcel, M. and Kępińska M. (2007). Kontrola procesu spawania TIG w oparciu o promieniowanie łuku spawalniczego. *Przegląd Spawalnictwa,* (12), pp. 15-20.
16. Whitaker, J.C. (2000). Signal measurement, analysis and testing. *CRC Press*, New York.
17. Moler, C.B. (2004). *Numerical Computing with Matlab*. Chapter V: Least Squares. Society for Industrial and Applied Mathematics.
18. Madansky, A. (1988). *Prescriptions for working statisticians*. Springer-Verlag, New York.